The Impacts of Adhesion on the Wear Property of Graphene

Shuji Zhao, Zhihong Zhang, Zhanghui Wu, Kaihui Liu, Quanshui Zheng, and Ming Ma*

Adhesion plays an important role in the antiwear property of graphene layer on a substrate. Here the wear property of the inner region of monolayer graphene grown on copper foils via chemical vapor deposition is studied. The adhesive strength is controlled by changing the oxidation of the copper substrate into two oxidation degrees with intact graphene preserved. For graphene layers on copper substrates with either low oxidation degree (LOD) or high oxidation degree (HOD), it is found in both systems wear starts at the wrinkle position under similar normal force. However, with the development of wear, for the LOD substrate the covering graphene layer is worn out gradually, while for the HOD substrate the graphene layer is peeled off rapidly. By measuring the adhesion between graphene and substrates indirectly, together with finite element analysis, it is shown that the underlying mechanism for the different wear phenomena is due to the higher adhesion between graphene and LOD substrates than that between graphene and HOD substrates. This study provides insights on the impacts of adhesion between monolayer material and substrates on the antiwear properties, which can benefit the design of lubrication coatings based on layered materials.

1. Introduction

Graphene is an excellent lubricating coating layer[1] because of its extremely high intrinsic strength,[2] ultralow binding strength with many surfaces, e.g., graphite,[3] hexagonal boron nitride (hBN),[4] MoS_2,[5] and atomically smooth surface.[6] For example, the friction between graphene/graphene,[3,7–9] graphene/MoS_2,[7] graphene/hBN,[4,7,8] and graphene/diamond-like-carbon (DLC)[10] measured at either nanoscale[7] or microscale[3,4,8,10] could be so small that such layered-material junctions could reach superlubricity,

a state in which the lateral interactions between two incommensurate surfaces are effectively canceled resulting in ultralow sliding friction. The ultralow friction state could also be achieved for tip with radius from 20 to 1000 nm sliding on graphene supported by substrates, e.g., diamond tip with graphene on SiO_2 substrate,[11,12] Si tip with graphene on SiO_2 substrate,[13] and diamond tip with graphene on Cu substrate[14] and the lubrication properties was robust under different normal load.[15]

The ultralow friction and high intrinsic strength make graphene an ideal candidate for antiwear coating materials. On the nano and microlevel, Shin et al.[11] carried out microscale scratch tests on exfoliated and epitaxial graphene on a silica substrate. When the indenter was pressed into the monolayer graphene sample at a depth of more than 150 times of its thickness, no damage occurred within the graphene. Using atomic force microscope (AFM) tip with a radius about 100 nm sliding on graphene that mechanically exfoliated to SiO_2 substrates, Qi et al.[12] reported that the monolayer graphene still maintained a low friction coefficient of 0.01 for a prolonged period (4096 cycles) with a normal load up to 9150 nN, and the interior region of graphene shows better wear resistance. Qi et al.[16] further found that the wear resistance of the free edge of graphene could be improved by performing air plasma treatment. With a similar setup, Vasic et al.[17] showed that the SiO_2 substrate gets plastically deformed for lower normal loads, followed by a sudden

S. Zhao, Prof. M. Ma
State Key Laboratory of Tribology
Department of Mechanical Engineering
Tsinghua University
Beijing 100084, China
E-mail: maming16@tsinghua.edu.cn
S. Zhao, Z. Wu, Prof. Q. Zheng, Prof. M. Ma
Center for Nano and Micro Mechanics
Tsinghua University
Beijing 100084, China
Dr. Z. Zhang, Prof. K. Liu
State Key Laboratory for Mesoscopic Physics
School of Physics
Peking University
Beijing 100871, China

Dr. Z. Zhang
Academy for Advanced Interdisciplinary Studies
Peking University
Beijing 100871, China
Z. Wu, Prof. Q. Zheng
Department of Engineering Mechanics
Tsinghua University
Beijing 100084, China
Prof. K. Liu
Centre for Nanochemistry
College of Chemistry and Molecular Engineering
Peking University
Beijing 100871, China
Prof. K. Liu
Collaborative Innovation Centre of Quantum Matter
Beijing 100871, China

**ADVANCED
SCIENCE NEWS**
www.advancedsciencenews.com

**ADVANCED
MATERIALS
INTERFACES**
www.advmatinterfaces.de

tearing of graphene for high enough normal load, with subsequent graphene peeling off from the substrate. By transferring graphene grown on copper substrate by chemical vapor deposition (CVD) to SiO_2 substrate, Vasic et al.[18] further showed that the graphene was destroyed in the wrinkle areas when the normal force was only 1.5 µN. Besides the excellent lubrication properties, Klemenz et al.[19] found that the graphene cover could substantially enhance the load-carrying capacity of the Pt substrate. Zhang et al.[20] found that the wear resistance of graphene grain boundaries is closely related to the misorientation angle of grain boundaries and the wear resistance could be improved by strengthening the interfacial interaction between the graphene and underlying substrate.

On the macroscale, Huang et al.[14] carried out friction and wear experiments on graphene grown by CVD on copper foil using a sphere-on-flat reciprocating Nano Tribometer. By using a glass lens with a radius of 5 mm, the graphene layer did not get worn under a normal load of 0.1 mN (the corresponding Hertzian contact stress is 22 MPa) and the friction coefficient remained below 0.05. Graphene wear occurred when pressure was up to 0.5 mN. Berman et al.[21] found that the wear rate of iron balls in the hydrogen environment is much lower than that in the nitrogen environment when graphene coating is added because hydrogen atoms would combine with the dangling bond of graphene to prevent further wear. Romani et al.[22] reported that the friction force between the steel ball and steel surface can be largely reduced with graphene grown by CVD on the steel surface.

While there have been many studies about wear resistance of the graphene layer, as shown above, there is no study about the effect of adhesion between graphene and substrates on anti-wear properties of the inner region of graphene by changing the adhesion. To investigate such effect is important because, for coating materials like graphene, their adhesive strength to the substrates plays a crucial role in the dependence of friction force on the number of layers,[23–25] wear resistance of edge,[16] and contact configuration.[23] Thus, it is necessary to explore the relationship between the wear of graphene and the adhesion.

In this paper, we studied the wear properties of graphene on copper substrates with different oxidation degrees on micro-scale by AFM. We found that the graphene layer on copper with a low oxidation degree (LOD) was gradually removed by increasing the normal load. However, the wear rate of graphene on copper with a high oxidation degree (HOD) was much higher than that on the LOD substrate. The graphene layer got quickly peeled off along the damaged area in large flakes. By adhesion test using AFM, the adhesion force between graphene and HOD substrate was found to be smaller than that between graphene and LOD substrate. With finite element analysis, we found that the smaller adhesion between graphene and substrate was the reason for higher in-plane stress and out-plane stress during the wear tests, leads to the peeling off of graphene layer, resulting in faster wear rate.

2. Results and Discussion

Figure 1a shows the optical image of the specimen exposed to ambient condition for 6 months. The surface of copper without oxidation is white and the color of copper becomes deeper when it is oxidized.[26] Therefore, the red region corresponds to copper with a HOD, and the white region corresponds to LOD copper. The different oxidation degree of copper may be due to the different crystal orientation.[27] Obviously, the copper surface shows a nonuniform oxidation degree. This is further confirmed by measuring regions of the copper substrate in different colors using XPS. As shown in Figure 1b, compared to the LOD region, the Cu_2O content within the HOD region
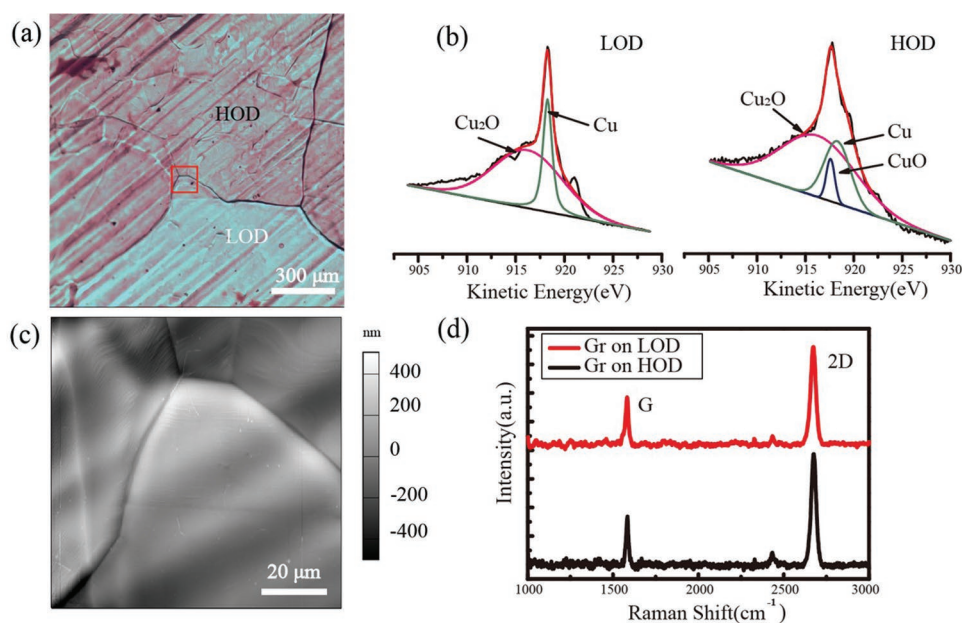

Figure 1. a) Optical image of the substrates. b) Results of XPS measurement on substrates with different oxidation degrees as labeled in (a). c) The AFM morphology image of substrates indicated in (a) by the red square. d) The Raman spectra of the graphene layers on substrates with different oxidation degrees.

increases, while the Cu content decreases and CuO presents. The morphology of the LOD and HOD regions as labeled by a red rectangle in Figure 1a is measured by AFM as shown in Figure 1c. Clearly, both regions show similar roughness. The quality of the graphene layer covering different regions was examined using Raman spectroscopy, with typical results shown in Figure 1d. In both cases, the Raman spectrum of graphene had no D peak, and the ratio of the intensity of G (1584 cm^{-1}) to 2D peak (2695 cm^{-1}) was around 1/2, indicating that the graphene on both substrates was of single layer and intact.

The wear tests on LOD and HOD substrates were carried out by scratching the graphene layer using the same AFM tip (DCP20). Within the same region scanned, the normal force was increased at intervals of 0.148 µN across different images. The corresponding normal contact stress estimated using Hertz theory[28] is from 3.59 to 9.89 GPa. As shown in **Figure 2a** (LOD) and Figure 2b (HOD), the friction first decreases slightly as the normal force increases, which is probably due to the gradual removal of surface contaminants and/or surface hardening of the substrate by plastic deformation.[12]

For the graphene layer, the presence of visible area with large friction indicates that those areas of graphene layer were worn. This is because the AFM tip started scratching the bare copper surface directly, and the friction became much larger than those areas covered by graphene due to the lubricating property of graphene.[14] Thus, for friction images as shown in Figure 2a–c, the worn areas are characterized by those regions correspond to high friction, i.e., brighter region. These worn areas are probably initiated during the wear process due to the stress concentration around the wrinkles[29] as indicated in Figure S1 in the Supporting Information. The wrinkles of graphene and the ripples which characterizing the morphology of copper substrate are both formed during the CVD progress.[30] From Figure 2a,b, it is evident that once the graphene layer got worn along with wrinkles, the wear rate of graphene on HOD substrate was much higher than that on LOD substrate with the increase of normal force. The additional wear tests on other LOD and HOD substrates with another DLC AFM tip show good reproducibility of the phenomenon observed (Figure S2, Supporting Information). By estimating the worn area quantitatively as shown in Figure 2d, the worn rate of the graphene layer on the HOD substrate is about one order higher than that on the LOD substrate. We further tested the upper limit of the wear resistance of those areas on graphene layer initially kept intact on the LOD substrate. This was done by selecting the intact region (area labeled by the green rectangle in Figure 2a) and performing wear test within these regions using higher normal load. As shown in Figure 2c, the graphene layer within this region could sustain a normal load up to ≈9 GPa before it got worn. For the stress concentration during wear test or the random defects in graphene introduced during the former wear progress, the graphene was worn on a certain point at the beginning.

Besides the quantitative difference of the wear processes of a graphene layer on the LOD and HOD substrate, we found that phenomenologically they are also different. As shown in Figure 2a, the worn area for the graphene layer on LOD substrates gradually extended along the damaged line, while on

HOD substrates the graphene layer was peeled along the damaged line in a form of large sheets (Figure 2b).

To estimate the influence of the wrinkles and ripples on the wear of graphene, we did wear tests on newly grown graphene by a CVD method on copper (Figure S3, Supporting Information). The wear processes with different densities of ripples are like those on LOD. But the critical normal load above which wear presents during the sliding process is significantly lower than that with sparse ripples (from 5.95 to 7.97 GPa). For graphene with denser ripples or wrinkles, it is reasonable to assume that more stress concentrated locations exist, thus easier to be worn during the wear tests. However, as shown in Figure S3 in the Supporting Information, for the substrate with the same oxidation degree, the difference in density of wrinkles/ripples would not change the form of wear qualitatively, e.g., either being peeled off or gradually removed.

The regions after wear tests were also characterized by Raman spectroscopy to find out the chemical changes. **Figure 3**a shows the optical image of the worn area on the LOD substrate. The dashed area corresponds to Figure 2a after all the wear tests were performed. The area highlighted by solid lines corresponds to Figure 2c. For those regions remain low friction (point 1), the presence of D and G peaks (Figure 3b) indicates that the graphene layer remained, but with defects. For point 2 which corresponds to the high friction region in Figure 2c, the absence of G peak shows that the graphene layer was completed destroyed. For the graphene layer on the HOD substrate, Figure 3c shows the optical image after the wear tests were performed. The region surrounded by the dashed lines corresponds to those areas shown in Figure 2b. The Raman spectroscope measured within the wear region shows no D and G peaks (point 3), indicating the absence of graphene layer after wear test. However, there were D, G, and 2D peaks appeared at the wear boundary (point 4), and the intensity of G peak is much larger than that of the 2D peak. This indicates that during the wear test, the graphene layer was pushed to the edge of the wear region and piled up.

The different wear rates and phenomena shown above indicate the governing factor for the wear process is quantitatively different. Previous studies on the friction of graphene on SiO$_2$ substrates indicate that the adhesion between the graphene layer and substrate plays a key role.[23] To this end, we estimated the adhesion between the graphene layer and substrates indirectly by measuring the adhesion force between the graphene layer and AFM tip on LOD and HOD substrates, with the mean pull-out force measured from five random selected points to be 38 ± 27 and 151 ± 30 nN, respectively. Because the adhesion between the tip and graphene is competitive with that between the substrate and graphene, the larger the adhesion between the tip and graphene is, the smaller the adhesion between graphene and the substrates is.[25] Therefore, the adhesion between graphene and the LOD substrates is larger than that between graphene and the HOD substrates. This experimental estimation is in accordance with earlier density functional theory results.[31] At the same time, the nanoscale trace–retrace images were obtained near the worn region on both substrates. **Figure 4**a,b is the nanoscale trace–retrace images obtained on LOD and HOD substrates. As shown by the images, the lateral force signal increased with the increase
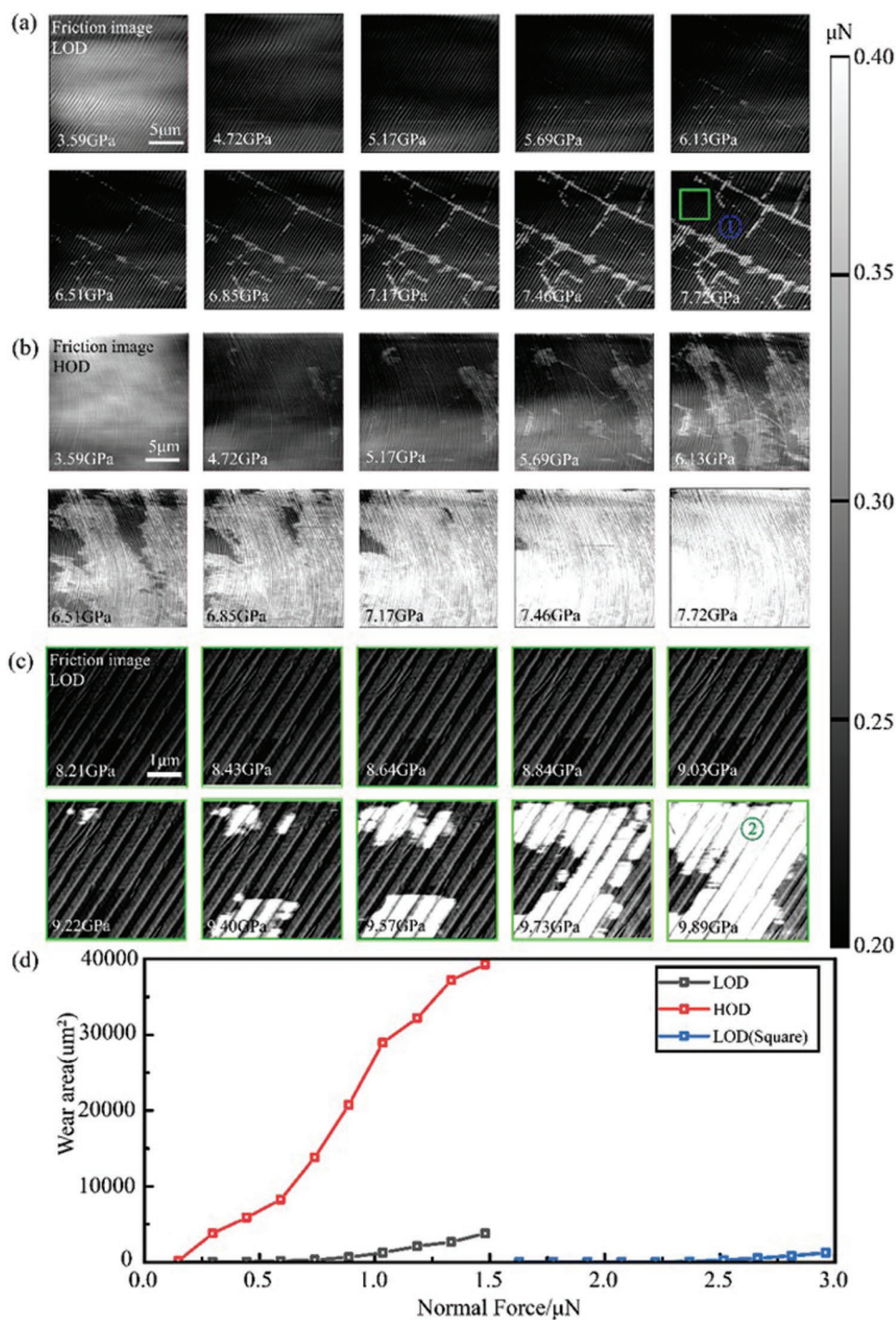
ADVANCED
SCIENCE NEWS
www.advancedsciencenews.com

ADVANCED
MATERIALS
INTERFACES
www.advmatinterfaces.de

Figure 2. a) Friction force images at the same location on LOD substrates, the normal force changed from 0.148 to 1.48 μN at intervals of 0.148 μN. The corresponding normal stress estimated from Hertz theory is marked within each image around the lower-left corner. b) Friction force images on HOD substrates. c) Friction force images measured within the white square area in (a), the normal force was further increased from 1.776 to 3.108 μN at intervals of 0.148 μN. d) Quantitative estimation of the worn area as shown in (a)–(c). The AFM topography of (a) and (b) at the beginning of the experiments is shown in Figure S1a,b of the Supporting Information.

of the moving distance on both substrates, but the increasing rate on HOD is larger. This larger increasing rate of lateral force means that graphene layer on HOD substrates is more prone to be wrinkled which resulting in stronger puckering effect that the contact area between AFM tip and graphene rose more quickly during sliding,[23,25,32] which supports the conclusion that the adhesion between graphene and HOD substrate is weaker.
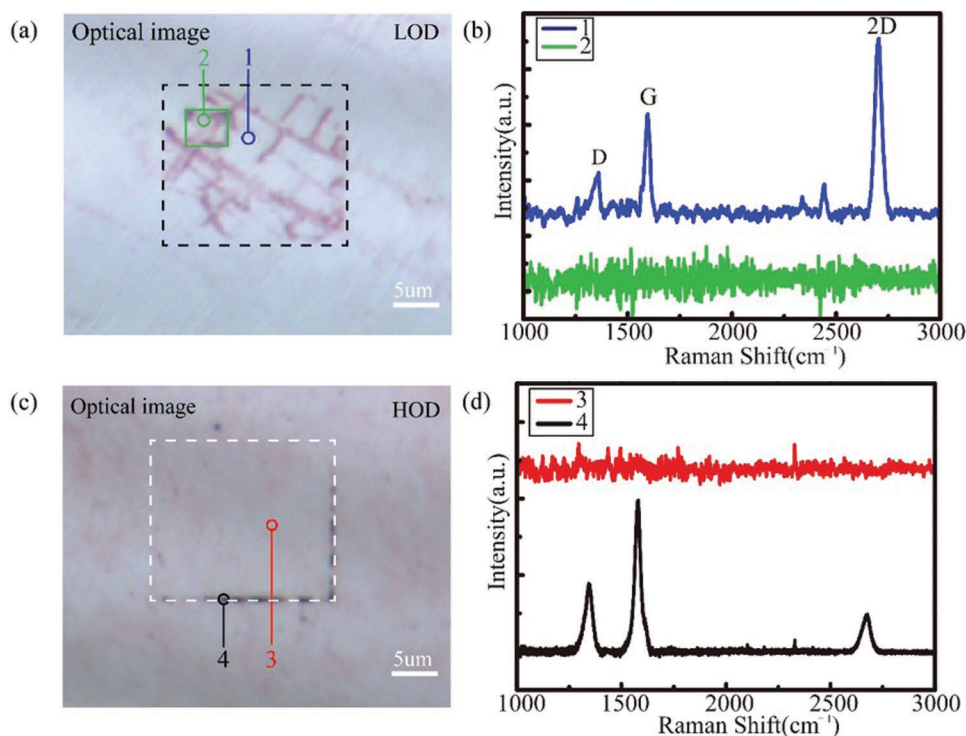
**ADVANCED
SCIENCE NEWS**
www.advancedsciencenews.com

**ADVANCED
MATERIALS
INTERFACES**
www.advmatinterfaces.de

Figure 3. a) Optical images of the worn area. The area marked in the dashed rectangle corresponds to those shown in the images in Figure 2a. The area labeled by a solid rectangle corresponds to those shown in Figure 2c. b) Raman spectra associated with those areas indicated in (a). c) Optical images of the worn area. The area marked in the dashed rectangle corresponds to those shown in the images in Figure 2b. d) Raman spectra associated with those areas indicated in (c).

To understand the relationship between wear and adhesion force in our experiments, we resorted to finite element simulations. Since on both LOD and HOD substrates, the wear of graphene layer happens first within the wrinkled area, we compared the sign of progress that the rigid ball moved from the edge of graphene to the inner region with different adhesion strength (0.05 and 0.5 J m^{-2}) as shown in **Figure 5**a. Since the surface is flat enough (Figure S1, Supporting Information) compared to the radius of the tip, we did not consider the influence of ripples in the simulation. The radius of the rigid ball was the 100 nm radius and half of the surface was covered with single layer graphene. The Young's Modulus and Poisson's ratio of Cu used in the simulation is 128 GPa and 0.34, respectively.[33] The effective Young's modulus, thickness, and Poisson's ratio of

graphene used is 5500 GPa, 0.066 nm, and 0.19, respectively.[34] As shown in Figure 5b, the maximum in-plane and out-plane stress of graphene during the movement on the high adhesion substrate (HAS) is smaller than that on the low adhesion substrate (LAS), which indicates that graphene is more easily broken on LAS at stress concentration point.

With the analysis shown above, the wear mechanism of graphene on copper can be deduced as shown in Figure 6. During the wear test, the graphene layer was damaged in the wrinkled area at first (**Figure 6**a). Because the strength of the step edge is much lower than that of the interior region,[12] the graphene layer got gradually peeled off along the damaged area. At the same time, in-plane defects and wear inevitably occur between the tip and graphene[12] (Figure 6b). Because
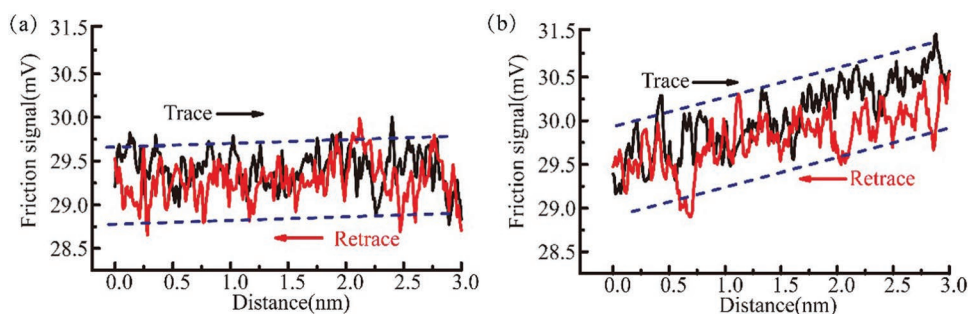

Figure 4. The trace–retrace images obtained on a) LOD and b) HOD substrates.

**ADVANCED
SCIENCE NEWS**
www.advancedsciencenews.com

**ADVANCED
MATERIALS
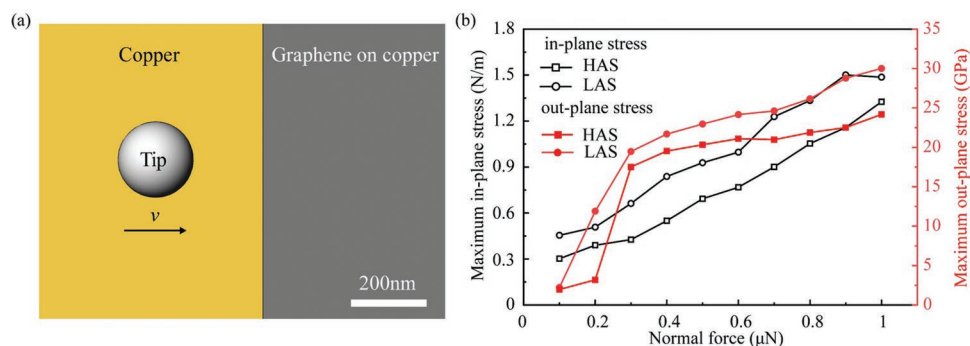INTERFACES**
www.advmatinterfaces.de

Figure 5. The finite element simulations of a rigid ball on graphene/copper. a) The schematic diagram of the simulation model. b) Maximum in-plane or out-plane stress in graphene when it is on high adhesion substrate (HAS) or low adhesion substrate (LAS) for a rigid ball moving from the edge of graphene to the inner of graphene under different normal load.

the adhesion between the LOD substrate and graphene is strong, there are low in-plane stress and out-plane stress. The exfoliation and damage of graphene become more difficult (Figure 6c). Experimentally it appears as in-plane wear and graphene were gradually worn along the failure line. However, the adhesion between the HOD substrate and graphene is weak, resulting in higher in-plane and out-plane stress within graphene. Therefore, the exfoliation and damage of graphene are easier (Figure 6d). So, the graphene on HOD substrates was damaged in the form of rapid exfoliation and the graphene sheets gathered at the edges of the wear test area.

3. Conclusion

Our experiments showed that the inner region of graphene exhibited better antiwear property on LOD substrates than HOD substrates. Specifically, the graphene layer was destroyed at the wrinkled area at first, and the damage of graphene on the LOD substrate developed slowly along the damaged line, while on the HOD substrate it expanded rapidly in the form of large sheets. By adhesion force tests and stick-slip images gotten by AFM, the adhesion between HOD substrates and graphene was found to be weaker than that between LOD substrates

and graphene. With finite element simulations, we found that graphene withstood higher in-plane and out-plane stress on the low adhesion substrates during the wear tests. Thus, we revealed that the rapid wear of graphene in the form of large sheets on the HOD substrate was due to the weak adhesion between graphene and substrate. Our study highlights the importance of adhesion on the in-plane wear of graphene and provides a possible direction to tune the antiwear properties of 2D materials on substrates.

4. Experimental Section

Using traditional CVD method,[35] single layer graphene was grown on copper foil of which the thickness was 25 μm. After exposing the specimen to the atmosphere for 6 months, the tribological characteristics of graphene were examined by AFM (Cypher ES, Oxford Instrument)under ambient conditions with a temperature of 25 °C and relative humidity around 30%. It is noticed that there are several methods reported to oxidize the copper substrates with a graphene coating, but they all introduce defects in graphene.[31,36] The wear and adhesion force tests were conducted with a DLC coated silicon AFM tip (NT-MDT, DCP20) in contact mode. The typical normal force constant of the tip was 48 N m⁻¹ and the tip radius was 100 nm. The normal force constant of the tip was calibrated by the noninvasive thermal calibration method described by Higgins et al.[37] The friction force was calibrated
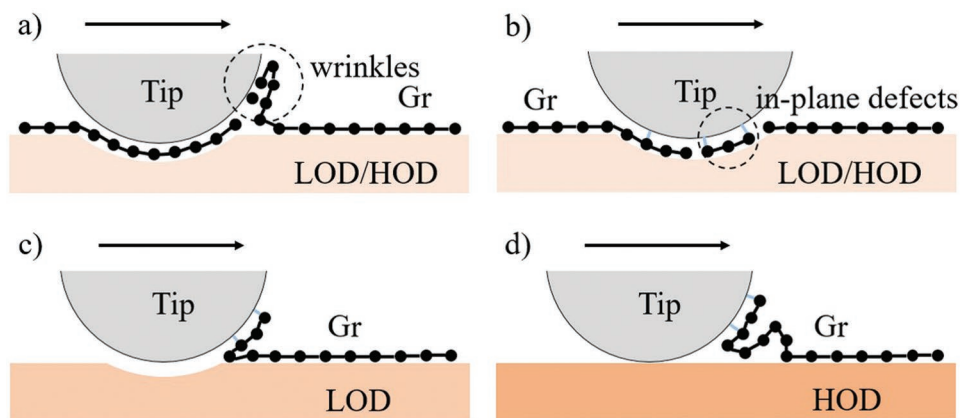

Figure 6. Schematic for the mechanism of wear. For both LOD and HOD substrates, a) graphene damages at the wrinkled area, and b) in-plane defects occur during the friction test will occur. However, c) graphene exfoliates slowly only happens for LOD substrates and d) graphene exfoliates quickly happens only for HOD substrates.

by the wedge calibration method introduced by Ogletree et al.[38] During the contact scanning process, the normal force was gradually increased to obtain friction images of graphene in the same region. Adhesive force tests were carried out by measuring the maximum force when the tip was pulled out of contact from the surface, with the normal force used for adhesion force measurement being 2 µN. The morphology of the surface was measured using a silicon probe (Mikro Masch, CSC37/No Al, Cantilever B) in contact mode. The frequency of AFM scanning for all tests was 1 Hz. Raman microscopy (LabRAM HR800, Horiba) was used to characterize the thickness of graphene under ambient conditions. The spatial resolution is 1 µm and the laser wavelength is 532 nm. The element composition of the substrate was characterized by X-ray photoelectron spectroscopy (XPS) (PHI Quantera II, Ulvac-Phi Inc). The XPS results were obtained in a vacuum (pressure less than 1×10^{-5} atm), and the diameter of the analysis area was 100 µm.

Supporting Information

Supporting Information is available from the Wiley Online Library or from the author.

Conflict of Interest

The authors declare no conflict of interest.

Keywords

[1] L. Liu, M. Zhou, L. Jin, L. Li, Y. Mo, G. Su, X. Li, H. Zhu, Y. Tian, *Friction* **2019**, *7*, 199.

[2] C. Lee, X. D. Wei, J. W. Kysar, J. Hone, *Science* **2008**, *321*, 385.

[3] Q. S. Zheng, B. Jiang, S. P. Liu, Y. X. Weng, L. Lu, Q. K. Xue, J. Zhu, Q. Jiang, S. Wang, L. M. Peng, *Phys. Rev. Lett.* **2008**, *100*, 067205.

[4] Y. Song, D. Mandelli, O. Hod, M. Urbakh, M. Ma, Q. Zheng, *Nat. Mater.* **2018**, *17*, 894.

[5] L. Wang, X. Zhou, T. Ma, D. Liu, L. Gao, X. Li, J. Zhang, Y. Hu, H. Wang, Y. Dai, J. Luo, *Nanoscale* **2017**, *9*, 10846.

[6] C. C. Vu, S. M. Zhang, M. Urbakh, Q. Y. Li, Q. C. He, Q. S. Zheng, *Phys. Rev. B* **2016**, *94*, 081405.

[7] Y. Liu, A. Song, Z. Xu, R. Zong, J. Zhang, W. Yang, R. Wang, Y. Hu, J. Luo, T. Ma, *ACS Nano* **2018**, *12*, 7638.

[8] S. W. Liu, H. P. Wang, Q. Xu, T. B. Ma, G. Yu, C. H. Zhang, D. C. Geng, Z. W. Yu, S. G. Zhang, W. Z. Wang, Y. Z. Hu, H. Wang, J. B. Luo, *Nat. Commun.* **2017**, *8*, 14029.

[9] Q. S. Zheng, Z. Liu, *Friction* **2014**, *2*, 182.

[10] Y. Gongyang, C. Y. Qu, M. Urbakh, B. G. Quan, M. Ma, Q. S. Zheng, *Friction* **2019**, https://doi.org/10.1007/s40544-019-0288-0.

[11] Y. J. Shin, R. Stromberg, R. Nay, H. Huang, A. T. S. Wee, H. Yang, C. S. Bhatia, *Carbon* **2011**, *49*, 4070.

[12] Y. Z. Qi, J. Liu, J. Zhang, Y. L. Dong, Q. Y. Li, *ACS Appl. Mater. Interfaces* **2017**, *9*, 1099.

[13] a) L.-Y. Lin, D.-E. Kim, W.-K. Kim, S.-C. Jun, *Surf. Coat. Technol.* **2011**, *205*, 4864; b) Y. Peng, Z. Wang, K. Zout, *Langmuir* **2015**, *31*, 7782.

[14] Y. Huang, Q. Yao, Y. Qi, Y. Cheng, H. Wang, Q. Li, Y. Meng, *Carbon* **2017**, *115*, 600.

[15] a) P. Egberts, G. H. Han, X. Z. Liu, A. T. C. Johnson, R. W. Carpick, *ACS Nano* **2014**, *8*, 5010; b) M. Munther, T. Palma, A. Beheshti, K. Davami, *Mater. Lett.* **2018**, *221*, 54.

[16] Y. Z. Qi, J. Liu, Y. L. Dong, X. Q. Feng, Q. Y. Li, *Carbon* **2018**, *139*, 59.

[17] B. Vasic, A. Matkovic, U. Ralevic, M. Belic, R. Gajic, *Carbon* **2017**, *120*, 137.

[18] B. Vasic, A. Zurutuza, R. Gajic, *Carbon* **2016**, *102*, 304.

[19] A. Klemenz, L. Pastewka, S. G. Balakrishna, A. Caron, R. Bennewitz, M. Moseler, *Nano Lett.* **2014**, *14*, 7145.

[20] J. Zhang, X. Chen, Q. Xu, T. Ma, Y. Hu, H. Wang, A. K. Tieu, J. Luo, *Carbon* **2019**, *143*, 578.

[21] D. Berman, S. A. Deshmukh, S. K. R. S. Sankaranarayanan, A. Erdemir, A. V. Sumant, *Adv. Funct. Mater.* **2014**, *24*, 6640.

[22] E. C. Romani, D. G. Larrude, L. Nachez, C. Vilani, J. B. de Campos, S. B. Peripolli, F. L. Freire, Jr., *Tribol. Lett.* **2017**, *65*, 96.

[23] Q. Li, C. Lee, R. W. Carpick, J. Hone, *Phys. Status Solidi B* **2010**, *247*, 2909.

[24] a) X. Zheng, L. Gao, Q. Yao, Q. Li, M. Zhang, X. Xie, S. Qiao, G. Wang, T. Ma, Z. Di, J. Luo, X. Wang, *Nat. Commun.* **2016**, *7*, 13204; b) L. Fang, D.-M. Liu, Y. Guo, Z.-M. Liao, J.-B. Luo, S.-Z. Wen, *Nanotechnology* **2017**, *28*, 245703.

[25] X. Zeng, Y. Peng, H. Lang, *Carbon* **2017**, *118*, 233.

[26] a) Y. Zhang, H. Zhang, Z. Chen, X. Ge, Y. Liang, S. Hu, R. Deng, Y.-p. Sui, G.-h. Yu, *J. Appl. Phys.* **2017**, *121*, 245306; b) S. Chen, L. Brown, M. Levendorf, W. Cai, S.-Y. Ju, J. Edgeworth, X. Li, C. W. Magnuson, A. Velamakanni, R. D. Piner, J. Kang, J. Park, R. S. Ruoff, *ACS Nano* **2011**, *5*, 1321; c) F. Zhou, Z. Li, G. J. Shenoy, L. Li, H. Liu, *ACS Nano* **2013**, *7*, 6939.

[27] Y. Xu, J. Qu, Y. Shen, W. Feng, *RSC Adv.* **2018**, *8*, 15181.

[28] K. L. Johnson, *Contact Mechanics*, Cambridge University Press, Cambridge, UK **1985**, p. 90.

[29] F. Long, P. Yasaei, W. Yao, A. Salehi-Khojin, R. Shahbazian-Yassar, *ACS Appl. Mater. Interfaces* **2017**, *9*, 20922.

[30] a) K.-K. Bai, Y. Zhou, H. Zheng, L. Meng, H. Peng, Z. Liu, J.-C. Nie, L. He, *Phys. Rev. Lett.* **2014**, *113*, 086102; b) H. Zhang, Y. Zhang, B. Wang, Z. Chen, Y. Zhang, Y. Sui, G. Yu, Z. Jin, X. Liu, *RSC Adv.* **2015**, *5*, 96587.

[31] D. Luo, X. You, B.-W. Li, X. Chen, H. J. Park, M. Jung, T. Y. Ko, K. Wong, M. Yousaf, X. Chen, M. Huang, S. H. Lee, Z. Lee, H.-J. Shin, S. Ryu, S. K. Kwak, N. Park, R. R. Bacsa, W. Bacsa, R. S. Ruoff, *Chem. Mater.* **2017**, *29*, 4546.

[32] C. Lee, Q. Li, W. Kalb, X.-Z. Liu, H. Berger, R. W. Carpick, J. Hone, *Science* **2010**, *328*, 76.

[33] W. Martienssen, H. Warlimont, *Springer Handbook of Condensed Matter and Materials Data*, Springer, Berlin, Germany **2005**, p. 297.

[34] B. I. Yakobson, C. J. Brabec, J. Bernholc, *Phys. Rev. Lett.* **1996**, *76*, 2511.

[35] X. Xu, Z. Zhang, J. Dong, D. Yi, J. Niu, M. Wu, L. Lin, R. Yin, M. Li, J. Zhou, S. Wang, J. Sun, X. Duan, P. Gao, Y. Jiang, X. Wu, H. Peng, R. S. Ruoff, Z. Liu, D. Yu, E. Wang, F. Ding, K. Liu, *Sci. Bull.* **2017**, *62*, 1074.

[36] a) D. Dinh Loc, G. H. Han, S. M. Lee, F. Gunes, E. S. Kim, S. T. Kim, H. Kim, T. Quang Huy, K. P. So, S. J. Yoon, S. J. Chae, Y. W. Jo, M. H. Park, S. H. Chae, S. C. Lim, J. Y. Choi, Y. H. Lee, *Nature* **2012**, *490*, 235; b) Y. H. Wu, X. Y. Zhu, W. J. Zhao, Y. J. Wang, C. T. Wang, Q. J. Xue, *J. Alloys Compd.* **2019**, *777*, 135.

[37] M. J. Higgins, R. Proksch, J. E. Sader, M. Polcik, S. Mc Endoo, J. P. Cleveland, S. P. Jarvis, *Rev. Sci. Instrum.* **2006**, *77*, 013701.

[38] D. F. Ogletree, R. W. Carpick, M. Salmeron, *Rev. Sci. Instrum.* **1996**, *67*, 3298.